

Role of mitochondrial complex I and protective effect of CoQ₁₀ supplementation in propofol induced cytotoxicity

Christian Bergamini¹ · Noah Moruzzi² · Francesco Volta² · Laura Faccioli¹ · Jantje Gerdes² · Maria Cristina Mondardini³ · Romana Fato¹

Received: 16 June 2016 / Accepted: 2 August 2016 / Published online: 15 August 2016
© Springer Science+Business Media New York 2016

Abstract Propofol (2,6-diisopropylphenol) is an anaesthetic widely used for human sedation. Due to its intrinsic antioxidant properties, rapid induction of anaesthesia and fast recovery, it is employed in paediatric anaesthesia and in the intensive care of premature infants. Recent studies have pointed out that exposure to anaesthesia in the early stage of life might be responsible of long-lasting cognitive impairment. The apoptotic neurodegeneration induced by general anaesthetics (GA) involves mitochondrial impairment due to the inhibition of the OXPHOS machinery. In the present work, we aim to identify the main mitochondrial respiratory chain target of propofol toxicity and to evaluate the possible protective effect of CoQ₁₀ supplementation. The propofol effect on the mitochondrial functionality was assayed in isolated mitochondria and in two cell lines (HeLa and T67) by measuring oxygen consumption rate. The protective effect of CoQ₁₀ was assessed by measuring cells viability, NADH-oxidase activity and ATP/ADP ratio in cells treated with propofol. Our results show that propofol reduces cellular oxygen consumption rate acting mainly on mitochondrial Complex I. The kinetic analysis of Complex I inhibition indicates that propofol interferes with the Q module acting as a non-competitive inhibitor with higher affinity for the free form

of the enzyme. Cells supplemented with CoQ₁₀ are more resistant to propofol toxicity. Propofol exposure induces cellular damages due to mitochondrial impairment. The site of propofol inhibition on Complex I is the Q module. CoQ₁₀ supplementation protects cells against the loss of energy suggesting its possible therapeutic role to minimizing the detrimental effects of general anaesthesia.

Keywords Propofol · Complex I · Mitochondria · Anaesthesia · Oxygen consumption

Abbreviations

mPTP	Mitochondrial permeability transition pore
GA	General anaesthetics
PRIS	Propofol infusion Syndrome
CoQ ₁	2,3-Dimethoxy-5-methyl-6-(3-methyl-2-butenyl)-1,4-benzoquinone
DB	2,3-Dimethoxy-5-methyl-6-decyl-1,4-benzoquinone, oxidized form
DBH2	2,3-Dimethoxy-5-methyl-6-decyl-1,4-benzoquinol, reduced form
DCIP	2,6-Dichlorophenolindophenol
ETC	Electron Transfer Chain
BHM	Bovine Heart Mitochondria
TMPD	N,N,N',N'-Tetramethyl-p-phenylenediamine
FCCP	Carbonyl cyanide 4-(trifluoromethoxy) phenylhydrazone
FMN	Flavin mononucleotide
MTT	3-(4,5-Dimethyl-2-thiazolyl)-2,5-diphenyl-2H-tetrazolium bromide
TMRE	Tetramethylrhodamine ethyl ester
ECAR	Extracellular acidification rate
OCR	Oxygen consumption rate
OXPHOS	Oxidative phosphorylation

Electronic supplementary material The online version of this article (doi:10.1007/s10863-016-9673-9) contains supplementary material, which is available to authorized users.

✉ Romana Fato
romana.fato@unibo.it

¹ Department of Pharmacy and Biotechnology, University of Bologna, Via Imerio 48, Bologna, Italy

² Institute for Diabetes and Regeneration Research, Helmholtz Zentrum Munich, Parkring 11, 85478 Garching, Germany

³ Department of Paediatric Anaesthesia and Intensive Care, S. Orsola-Malpighi Hospital, Bologna University, Bologna, Italy

Introduction

Propofol is considered a safe agent for human sedation because of its peculiar intrinsic antioxidant capacity, its rapid induction (30–60 s.) and fast recovery of anaesthesia (4–6 min.) (Sebel and Lowdon 1989; Apfelbaum et al. 1993). Due to these features, propofol has also been frequently used in paediatric anaesthetic practice and in intensive care of premature infants (Istaphanous and Loepke 2009). However, emerging animal and human data suggest that high doses or prolonged exposure to propofol could damage the developing nervous system, raising serious questions regarding the safety of propofol for paediatric anaesthesia (Fredriksson et al. 2007; Cattano et al. 2008; Bercker et al. 2009; Istaphanous and Loepke 2009; Stratmann 2011; Zou et al. 2013).

Sporadically, propofol causes the so-called propofol infusion syndrome (PRIS), characterized by metabolic acidosis (Fodale and La Monaca 2008) resembling mitochondrial cytopathies and acquired carnitine deficiency (Marian et al. 1997; Wolf et al. 2001). These defects occur first in tissues with high-energy demand such as the heart and muscles. Notably, the use of propofol is discouraged in patients with mitochondrial diseases (Driessen et al. 2007; Schwartz and Raghunathan 2009). Consistently, it has been proposed that children who develop metabolic acidosis and myocardial failure after propofol infusion may have a subclinical form of mitochondrial disease (Parke et al. 1992). The neurotoxic effect of general anaesthetics (GA) results in an apoptotic loss of neurons and is accompanied by an impairment of synaptic development associated to modification of mitochondrial morphogenesis and function (Pearn et al. 2012).

Mitochondrial functionality and cellular energy content are considered important factors in cells survival; modifications of these factors can trigger apoptotic cell death. Apoptotic neurodegeneration and neurobehavioral deficits are mainly observed in animals or humans undergoing general anaesthesia by propofol during the period of brain growth known as “brain growth spurt” (a period that occurs from the foetal development until to about 2 years after birth for humans and 2 or 3 weeks after birth in mice and rats) (Dobbing and Sands 1979). During the brain growth spurt the energy demand is extremely high and even a partial reduction of energy supplies can have a strong impact on neural development. Retrospective studies on children exposed to general anaesthesia, as well as the results obtained in new-born animals, showed a toxic effect of the anaesthetic on the brain development that results in long-lasting cognitive impairment (Jevtovic-Todorovic et al. 2003; Fredriksson et al. 2004; Fredriksson et al. 2007; Wilder et al. 2009; Paule et al. 2011; Block et al. 2012; Boscolo et al. 2012).

The mitochondrial impairment after propofol administration has been investigated on several experimental models

often leading to different and opposite results (Boscolo et al. 2012). Propofol treatment on rat liver isolated mitochondria resulted in impairment of mitochondrial function on several levels: respiratory chain inhibition, ATPase impairment (Marian et al. 1997), direct effect on mPTP (Sztark et al. 1995; Javadov et al. 2000; Twaroski et al. 2015) and uncoupling of the respiratory chain (Branca et al. 1995; Sztark et al. 1995; Schenkman and Yan 2000; Wu et al. 2005). Moreover, abnormalities in plasma concentration of malonylcarnitine and C5-acylcarnitine in a child treated with propofol have been reported. This suggests an inhibitory effect of propofol on the carnitine palmitoyl transferase 1, thus leading to an impaired fatty-acid oxidation and ATP production (Fodale and La Monaca 2008). Recently, Vanlander et al. showed that in liver mitochondria enriched fractions from rat sedated with propofol, Complex II + III activity, but not the activity of the single complexes, was strongly decreased, pointing out an interference with the Coenzyme Q pool. Moreover, a decreased activity in Complex II + III was detected in skeletal muscle homogenate from one patient which died during the acute phase of PRIS (Vanlander et al. 2015). To clarify the effect of propofol on mitochondrial respiratory chain we used both intact cells and isolated mitochondria. In particular, we investigated the sites of propofol inhibition on mitochondrial Complex I and proposed an inhibition mechanism. Since the physiological substrate of mitochondrial Complex I is Coenzyme Q₁₀ (CoQ₁₀), we investigate the possible protective role of CoQ₁₀ supplementation on cultured cells exposed to propofol.

Materials and methods

Chemicals

All chemicals were purchased from Sigma (St. Louis, MO, USA) unless stated otherwise.

Cell culture

HeLa cells and T67 cells (Lauro et al. 1986) were cultured in DMEM (PAA, DASIT, Milan, Italy) supplemented with 2 mM L-glutamine, 10 % (v/v) foetal bovine serum (FBS), 100 U/mL penicillin and 100 µg/mL streptomycin at 37 °C in humidified atmosphere with 5 % CO₂. Culture medium was changed every 2 days and sub-confluent cells were splitted using 0.05 % trypsin–EDTA solution.

Bovine heart mitochondria isolation

Bovine heart mitochondria (BHM) were isolated according to Smith, A.L. (Smith 1967) with modifications to allow large-scale isolation (Pallotti and Lenaz 2007). Protein content was

measured by the Biuret method of Gornall et al. (Gornall et al. 1949) with addition of 10 % sodium deoxycholate using bovine serum albumin (BSA) as standard. BHM were stored at -80°C . BHM were frozen and thawed three times before use to avoid compartmentalization.

Mitochondrial oxygen consumption

BHM were assayed for oxygen consumption using a thermostatically controlled oxygraph chamber (Instech Mod.203, Plymouth Meeting, PA, USA) in 1.5 ml of incubation medium containing: KCl 50 mM, TRIS 10 mM, MgCl_2 3 mM, EDTA 1 mM, BSA 0.5 mg/ml pH 7.4, using 1 mg of mitochondrial protein/ml. BHM were incubated for 5 min with different propofol concentrations (up to 100 μM) and NADH 200 μM , succinate 20 mM, reduced decylubiquinone 100 μM and ascorbate-N,N,N',N'-Tetramethyl-p-phenylenediamine (TMPD) (respectively 10 mM and 400 μM) were added to start the reaction respectively from Complex I, II, III and IV. Rotenone, Antimycin A and KCN were added at the end of experiments to inhibit specifically Complex I, III and IV respectively. The respiratory rates were expressed in $\mu\text{mol O}_2/\text{min}/\text{mg}$ of protein referring to 250 nmol O_2/ml of buffer as 100 % at 30°C (Estabrook 1967).

Spectrophotometric analyses of respiratory chain enzymes

The activities of the respiratory chain complexes were measured using an ultraviolet/visible spectrophotometer (Jasco V-550) equipped with thermostatic control and cuvette stirring. NADH-CoQ₁ and NADH-DB reductase were measured according to Estornell et al. (Estornell et al. 1993). Quinone concentration was determined spectrophotometrically using $\epsilon_{275\text{nm}} = 13.7 \text{ mM}^{-1} \text{ cm}^{-1}$ for CoQ₁ and $\epsilon_{275\text{nm}} = 14 \text{ mM}^{-1} \text{ cm}^{-1}$ for DB.

NADH-DCIP (2, 6-Dichloroindophenol) activity was measured according to Fato et al. (Fato et al. 2009). NADH-ferricyanide ($[\text{Fe}(\text{CN})_6]^{3-}$) activity was measured according to Fato et al. (Fato et al. 1996). Briefly, the NADH-ferricyanide reductase activity was assayed at $\lambda = 420 \text{ nm}$, using $\epsilon_{420\text{nm}} = 1 \text{ mM}^{-1} \text{ cm}^{-1}$. The specific activity of NADH-ferricyanide reductase in the presence of 2 mM potassium ferricyanide was used to estimate the content of active Complex I in BHM by considering half of the maximal turnover as $8 \times 10^5 \text{ min}^{-1}$ (Cremona and Kearney 1964) since the concentration of ferricyanide was approximately equal to the K_m (Smith et al. 1980; Degli Esposti et al. 1994).

The NADH- O_2 activity in cellular homogenate was measured by following the decrease in absorbance due to the oxidation of NADH at 340 nm. Briefly, cells were homogenate by means of a Dounce homogenizer in hypotonic medium consisting of 100 mM KCl, 10 mM TRIS, 1 mM EDTA,

and 0.5 % bovine serum albumin (BSA) pH 7.2. The cell homogenate was frozen and thawed three times to avoid mitochondrial compartmentalization. The reaction buffer consisted of 50–100 μg of cellular homogenate, 25 mM potassium phosphate, 5 mM MgCl_2 , pH 7.2, 30°C . The reaction started by adding 100 μM of NADH; 0.5 μM rotenone was added at the end of experiments to completely inhibit Complex I (Pallotti and Lenaz 2007).

XF extracellular flux analysis

Metabolic analysis was performed using Seahorse XF96 Flux Analyser (Seahorse Biosciences, Billerica, MA, USA). 20,000 cells/well were seeded the day before the experiment. The day of the experiment the growing medium was replaced with XF medium 5.5 mM glucose, containing 2 mM GlutaMax (Gibco), 1 mM sodium pyruvate and 1 % FBS. Cells were incubated at 37°C without CO_2 for 1 h prior to the experiment. We measured the oxygen consumption (OCR) and extracellular acidification (ECAR) rates before and after addition of propofol (2.5–50 μM) and oligomycin (1 μM). Equal amounts of DMSO have been used in the injections of propofol and control (<1 % final concentration). Data are presented as ratio against basal OCR and ECAR.

Mitochondrial transmembrane potential ($m\Delta\psi$)

Transmembrane potential was measured using a SP5 confocal microscope (Leica, Mannheim, Germany) with a heated stage. 200,000 cells/well in a glass bottom 24 multiwell plate were seeded the day before. On the day of the experiment the growth medium was replaced with XF media as described above, containing 500 nM tetramethyl-rhodamine-ethyl-ester (TMRE, Molecular probes). Microscope settings: Obj. 10 \times , 4 % laser power, 512×512 pixel, λ_{ex} 514 nm and λ_{em} 565/600 nm, pinhole 1 Airy, Optimized Z stack. Images were analysed with Imaris 7.4.5 software (Bitplane AG, Zurich, Switzerland). Total intensity of the identified objects per field (above 10 voxels) was divided for total objects volume. For each sample, two different fields were averaged.

Cell viability assay

Propofol cytotoxicity was estimated using MTT (Thiazolyl Blue Tetrazolium Bromide) assay. HeLa and T67 cells were seeded in 24-well plates and cultured overnight. The subsequent day, cells were washed with PBS and incubated with propofol (ranging from zero to 100 μM) dissolved in complete DMEM for 24 h. After incubation time, cells were carefully washed with PBS and incubated for 3 h with 500 μM MTT dissolved in DMEM. Then, cells were washed with PBS and lysed with 200 μL of dimethyl sulfoxide. Equal amounts of DMSO have been used in propofol treated samples and

control (<1 % final concentration). The absorbance of each well was measured at 595 nm using a microplate reader (Victor² 1420 multilabel counter, Perkin Elmer). All data points were performed in triplicate with a minimum of $n = 3$.

ATP and ADP determination

Nucleotides were extracted and detected as described by Jones DP. (Jones 1981) using a Kinetex C18 column (250 × 4.6 mm, 100 Å, 5 µm; Phenomenex, CA, USA), with a two pump Agilent 1100 series system. Absorbance (260 nm) was monitored with a photodiode array detector (Agilent 1100 series system). Nucleotide peaks were identified by comparison and coelution with standards and quantification by peak area measurement compared with standard curves.

Extraction and quantification of coenzyme Q

Extraction of coenzyme Q from cultured cells was performed as described by Takada et al. (Takada et al. 1984). Quantification of CoQ₁₀ was performed by HPLC analysis using a two pump Agilent 1100 series system. Absorbance (275 nm) was monitored with a photodiode array detector (Agilent 1100 series system). 20 µl of ethanolic extract was chromatographed on a C18 column (Kinetex, Phenomenex, 2.6 µm, 100 × 4.6 mm), using a mobile phase consisting of ethanol: water (97 : 3, v/v) at a flow rate of 0.4 ml/min. The concentrations of CoQ₁₀ were obtained by comparison of the peak areas with those of standard solutions.

Results

Propofol inhibits oxygen consumption in cultured cells and in BHM

Effect of propofol treatment on HeLa cells

One of the effects associated to the propofol infusion syndrome is the induction of lactic acidosis (Koch et al. 2004; Haase et al. 2005) which suggests an impairment of the mitochondrial respiratory chain and a cellular compensation of ATP production through glycolysis. Therefore, we monitored the oxygen consumption rate (OCR) and extracellular acidification rate (ECAR) in HeLa cells after acute treatment with propofol (up to 50 µM). As expected, the addition of propofol induced a significant dose dependent decrease in OCR (Fig. 1a, b) and a parallel increase in ECAR (Fig. 1c, d). Notably, only minimal effect on mitochondrial potential was observed 10 min after the addition of 50 µM of propofol (Fig. 1e). Considering the cellular difficulties to cope with a mitochondrial impairment, we measured the cytotoxic effect of propofol on HeLa cells. After 24 h of treatment,

we observed a significant dose-dependent decrease of cell viability (Fig. 1f).

Effect of propofol treatment on oxygen consumption in isolated mitochondria

To study the effect of propofol on the mitochondrial respiratory chain we decided to test the effect of propofol exposure directly on isolated mitochondria. Beef Heart Mitochondria (BHM) are a well-established model to study the effect of compounds interfering with the enzymes of the respiratory chain. We measured the effect of propofol on oxygen consumption in BHM in the presence of different respiratory substrates: NADH, succinate, DBH₂ and ascorbate/TMPD, respectively oxidized at the level of Complex I, II, III and IV. The NADH-O₂ reductase activity was 0.334 ± 0.013 µmoles O₂ min⁻¹ mg⁻¹ and it was already significantly reduced following addition of 10 µM of propofol (0.263 ± 0.005 µmoles O₂ min⁻¹ mg⁻¹) (Fig. 2a) whereas the succinate-O₂ activity (0.052 ± 0.006 µmoles O₂ min⁻¹ mg⁻¹ in untreated BHM) was only slightly reduced, in fact, the maximal extent of propofol inhibition did not exceed 15 % (Fig. 2b). The DBH₂-O₂ activity (Fig. 2c) was 0.716 ± 0.079 µmoles O₂ min⁻¹ mg⁻¹ and it was significantly reduced only in the presence of 50 µM propofol (0.582 ± 0.073 µmoles O₂ min⁻¹ mg⁻¹). The ascorbate/TMPD-O₂ activity (Fig. 2d) was not altered (0.711 ± 0.011 µmoles O₂ min⁻¹ mg⁻¹ in the presence of 100 µM propofol vs. 0.732 ± 0.010 µmoles O₂ min⁻¹ mg⁻¹ in untreated BHM). Moreover, we have found that propofol does not affect Complex II activity measured as Succinate-Q₁-DCIP (data not shown).

Taken together, these data suggest that propofol acts mainly on Complex I and III. The effect of propofol on the respiratory chain is maximum when Complex I is the electron entry point and for this reason it can be inferred that the Complex I is the main target for the propofol inhibition within the ETC.

Effect of propofol on mitochondrial complex I

Figure 3 reports the effect of propofol treatment on the Complex I reductase activity measured in the presence of different exogenous electron acceptors. We observed that the NADH-[Fe(CN)₆]³⁻ as well as the NADH-DCIP oxidoreductase activity were not modified by concentrations of propofol up to 100 µM (Fig. 3a, b), while the NADH-CoQ₁ oxidoreductase activity was strongly affected by propofol exposure (Fig. 3c). The lack of inhibition of the NADH-ferricyanide and NADH-DCIP reductase activity allowed us to exclude the FMN as site of propofol interaction on Complex I. Furthermore, the significant and dose-dependent decrease of the NADH-CoQ₁ reductase activity (Fig. 3c) indicates that the inhibitory mechanism involves the physiological quinone reducing site on Complex I.

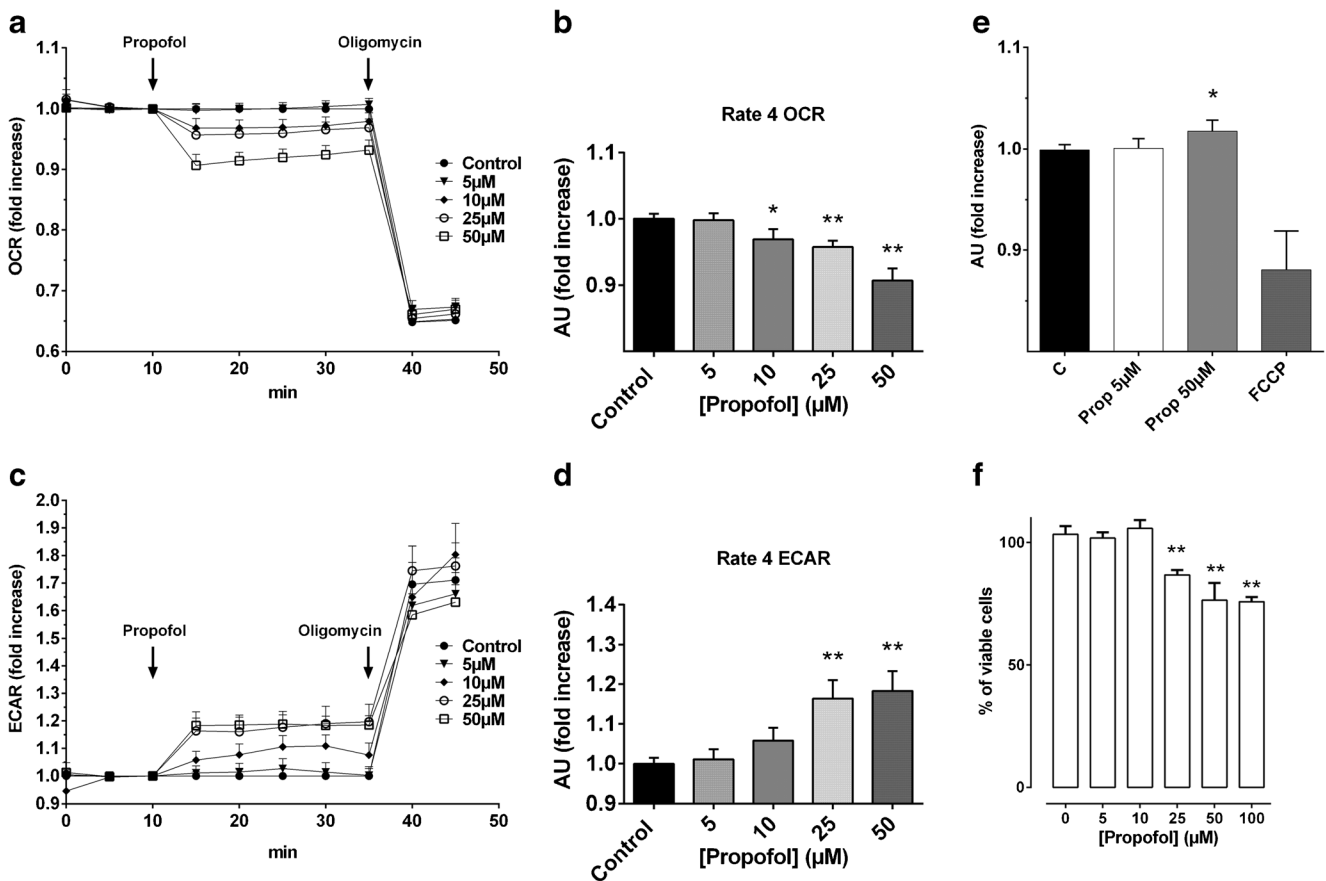


Fig. 1 a–f Effect of propofol on HeLa cells. **a, b** Oxygen consumption rate (OCR) and (**c, d**) extracellular acidification rate (ECAR) measured with flux analysis in HeLa cells after acute propofol exposure. ATP coupled respiration was blocked using 1 μ M Oligomycin ($n = 25$). **e** Effect of propofol exposure on mitochondrial potential, 2.5 μ M FCCP

was added as uncoupler ($n = 12$). **f** Effect of 24 h of propofol incubation on HeLa cells viability measured by MTT assay ($n = 4$). Data are expressed as mean \pm SE. Significance was determined by ANOVA and Tukey analysis between treated cells and controls. * $P \leq 0.05$, ** $P \leq 0.01$

Kinetic analysis of propofol inhibition of NADH-CoQ reductase activity in BHM

The Michaelis-Menten plots for NADH-CoQ₁ and NADH-DB reductase activities (Fig. 4a, b) showed that propofol treatment induced a decrease in the maximal velocity (V_{max}) and a parallel increase in the Michaelis-Menten constant (K_m) values suggesting a non-competitive inhibition mechanism.

The non-competitive behaviour for propofol inhibition becomes more evident when the data are represented in a Lineweaver-Burk plot (Fig. 4c-d). The intersection points in the graphs are located above the x-axis (IV quadrant) suggesting a non-competitive mechanism with a higher affinity of the inhibitor for the free form of the enzyme.

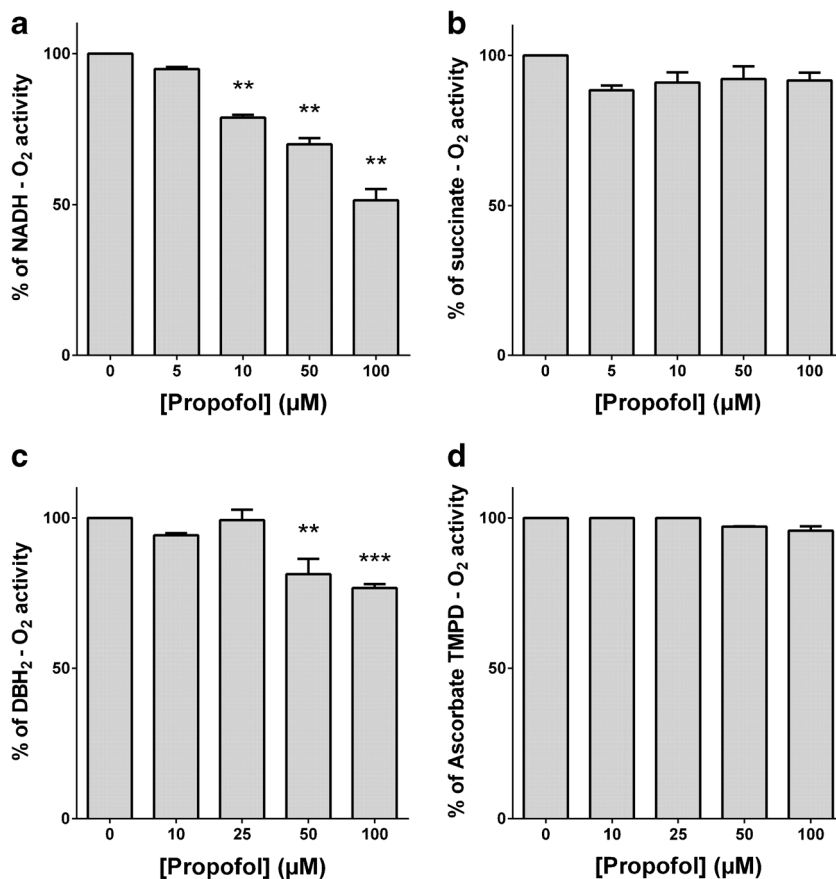
Table 1 reports the effect of propofol on the catalytic efficiency (k_{cat}/K_m) of Complex I measured in BHM in the presence of DB or CoQ₁. The k_{cat} values were determined by the maximal velocity derived from the Michaelis-Menten analysis, referred to mitochondrial Complex I content (25 pmol/mg of total mitochondrial protein) estimated by NADH-[Fe(CN)₆]³⁻

reductase activity. (Cremona and Kearney 1964; Smith et al. 1980; Degli Esposti et al. 1994).

We observed a reduction of Complex I catalytic efficiency of 72 % and 75 % respectively for the NADH-DB and NADH-CoQ₁ reductase activity. Complex I activity rates in the presence of propofol never approach zero, suggesting a partial non-linear inhibition mechanism (for details see Fig.1 Supplementary Material). We have recalculated the data reported in Fig. 4c and d to obtain the kinetic parameters α and β according to Leskovac (Leskovac 2003) (For details, see Fig. 2 Supplementary Material). The α value represents the effect of propofol on the association constant (K_m) of the substrate (DB or CoQ₁) to the EI complex, as well as the effect on the K_i value for the inhibitor binding to ES complex. The β value defines the effect of the inhibitor on the catalytic constant (k_{cat}).

The α and β values calculated using DB are: $\alpha = 2.25$ and $\beta = 0.146$. In the presence of CoQ₁, we obtained: $\alpha = 0.455$ and $\beta = 0.037$. These values are consistent with a non-competitive mechanism of inhibition. Nevertheless, the α

Fig. 2 a-d Effect of Propofol on mitochondrial electron transfer chain. Polarographic measurements of oxygen consumption in BHM treated with propofol. **a** NADH-O₂ activity (I + III + IV), **(b)** succinate-O₂ activity (II + III + IV), **(c)** DBH₂-O₂ activity (III + IV) and **(d)** ascorbate TMPD-O₂ activity (IV). The specific activities I + III + IV, II + III + IV and III + IV were assessed by adding 2 μM antimycin A at the end of experiments. Complex IV specific activity was assessed using 2 mM KCN at the end of experiments. Data are expressed as percentage of enzyme activity ± SE from at least three independent experiments. Significance was determined by ANOVA and Tukey analysis between treated cells and controls. ** $P \leq 0.05$, *** $P \leq 0.01$



value in the presence of DB is >1 , indicating that the inhibitor binds preferentially to the free enzyme. When using CoQ₁ the α value is <1 which is consistent to a greater affinity of the inhibitor to the ES complex, suggesting an uncompetitive mechanism. This discrepancy might be due to the different interaction of short chain quinones with Complex I as suggested by the different rotenone sensitivity and by the different partition coefficient ($\log P$ membrane/water = 2.9 and 4.7 for CoQ₁ and DB respectively (Fato et al. 1996)).

Protective effect of CoQ₁₀ administration on propofol induced cellular toxicity

Cell viability

Our data suggest that propofol can have a direct inhibitory effect on the mitochondrial Complex I interfering with the quinone-binding site. Even though the inhibition mechanism derived from kinetic analysis looks non-competitive, the α

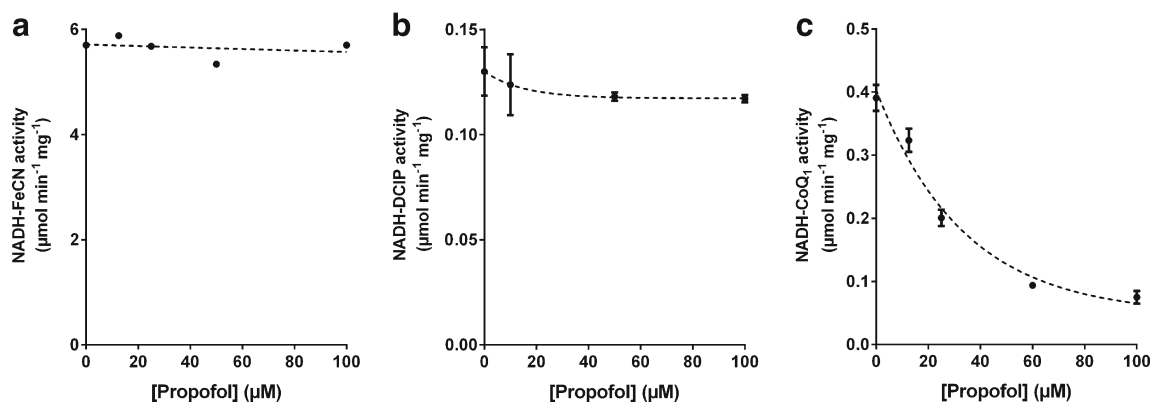


Fig. 3 a-c Effect of propofol on Complex I activity. Mitochondrial Complex I was functionally isolated in BHM using 2 μM Antimycin A and 2 mM KCN. The NADH oxidation by Complex I was followed spectrophotometrically at 340 nm using as hydrophilic electron acceptors:

(a) 2 mM [Fe(CN)₆]³⁻, (b) 50 μM DCIP and (c) 50 μM DCIP in the presence of 75 μM CoQ₁. Data are expressed as μmol min⁻¹ mg⁻¹ ± SE from at least three independent experiments

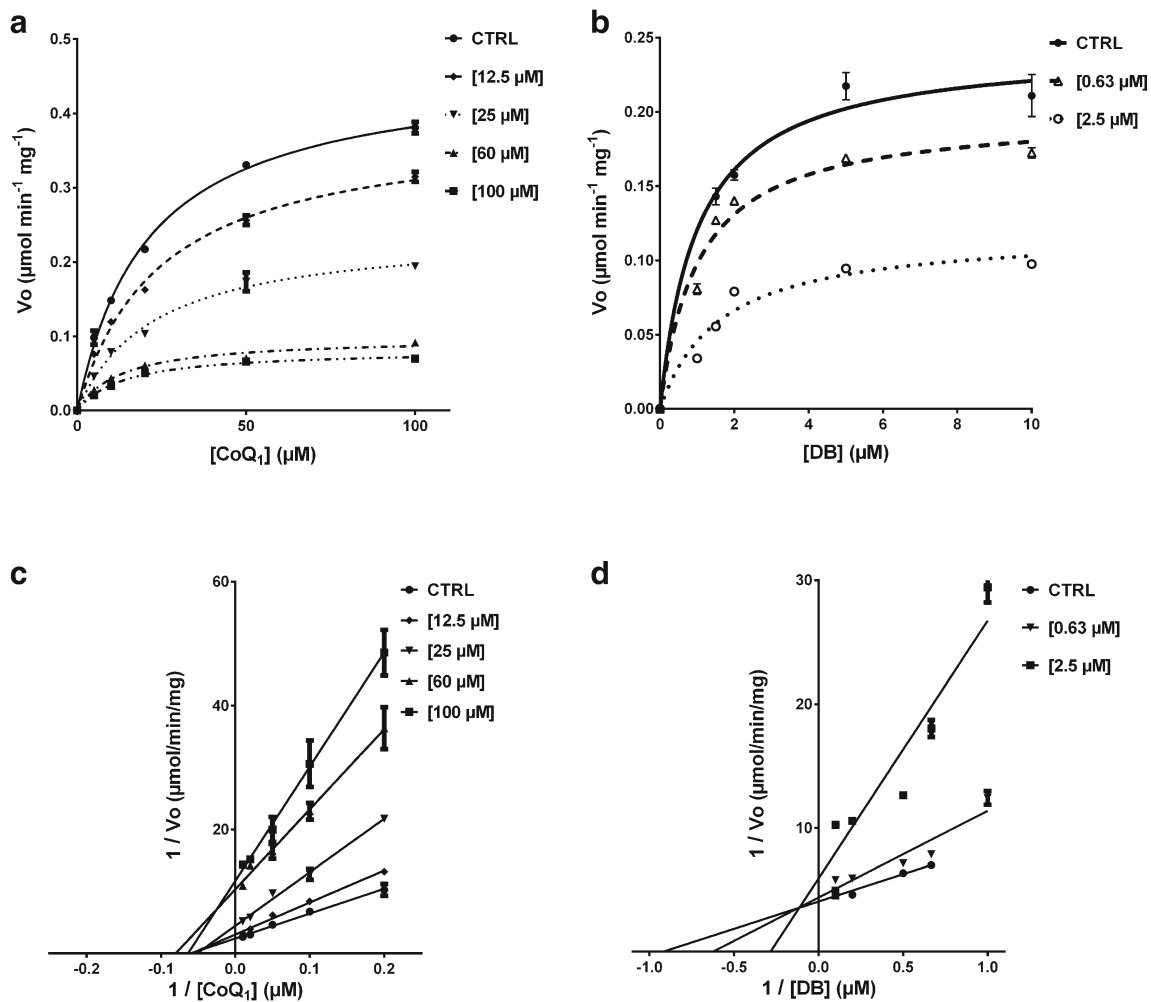


Fig. 4 a-d Kinetic analysis of Complex I using CoQ₁ and DB. The Complex I activity in BHM measured in the presence of fixed propofol concentrations by titrating the electron acceptor CoQ₁ (a) and Decylubiquinone (DB) (b). Mitochondrial Complex I was functionally isolated in BHM using 2 μM Antimycin A and 2 mM KCN. The NADH oxidation by Complex I was followed spectrophotometrically at 340 nm.

Data are expressed as μmol min⁻¹ mg⁻¹ ± SD from at least three independent experiments. **c** Lineweaver–Burk plot of NADH–CoQ₁ titration and **(d)** Lineweaver–Burk plot of NADH–DB titration. Each point is the average ± SD of at least three different determinations. The r square values for the linear fitting of Lineweaver–Burk plots are >0.97 for NADH–CoQ₁ and >0.90 for NADH–DB

Table 1 Catalytic efficiency values for NADH–DB and NADH–CoQ₁ activities in the presence of different propofol concentrations. Complex I content in BHM was 25pmoles/mg of total protein as estimated by NADH–[Fe(CN)₆]³⁻ activity (see [Material and Methods](#) section)

Propofol μM	k _{cat} /K _m (NADH–DB oxidoreductase) M ⁻¹ min ⁻¹	k _{cat} /K _m (NADH–CoQ ₁ oxidoreductase) M ⁻¹ min ⁻¹
0	18.16*10 ⁷	1,52* 10 ⁷
0.63	13.54*10 ⁷	
2.5	5.02*10 ⁷	
12.5		1,06 * 10 ⁷
25		0,70 * 10 ⁷
37		0,60 * 10 ⁷
60		0,48 * 10 ⁷
100		0,38 * 10 ⁷

values are consistent with a higher affinity of the inhibitor for the free enzyme in comparison to the enzyme–substrate complex. This last observation suggests that increasing the natural substrate (CoQ₁₀) of the complex I could reduce the affinity of the enzyme for propofol, resulting in a decreased toxicity.

In order to verify this hypothesis we have supplemented cells prior propofol treatment with 100 nM of a water-soluble and more bioavailable formulation of CoQ₁₀ named Q_{Ter}[®] (Bergamini et al. 2012; Fetoni et al. 2013). To note, the total CoQ₁₀ content after treatment with Q_{Ter}[®] is approximately 20 folds higher compared to untreated cells (Fig. 6c). Here, we found that cells viability of T67 and HeLa cell lines treated with propofol concentrations ranging from 10 to 25 μM is rescued in the presence of CoQ₁₀ (Fig. 5). However, at higher concentrations of the anaesthetic the CoQ₁₀ is not able to protect from the cytotoxic effect of propofol.

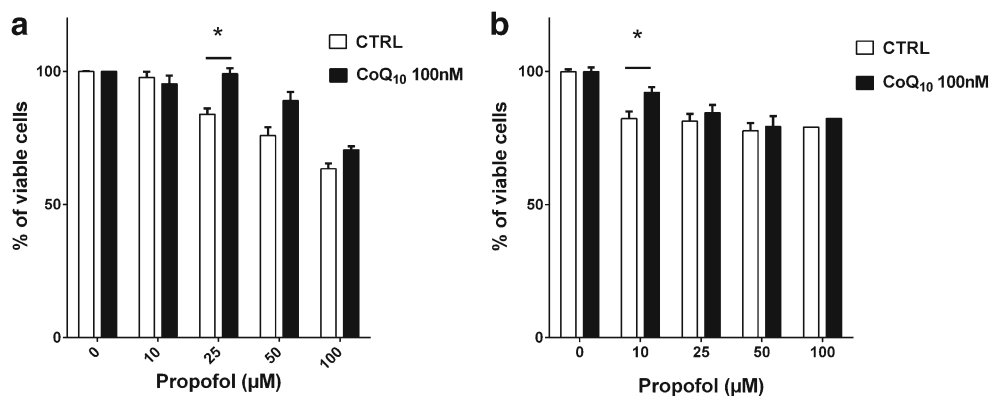


Fig. 5 a-b Effect of propofol treatment on T67 (panel a) and HeLa (panel b) cells viability. Cells were preincubated for 24 h with 100 nM of terclatrated Coenzyme Q or vehicle (CTRL), and then cells were treated for 24 h with different concentrations of propofol.

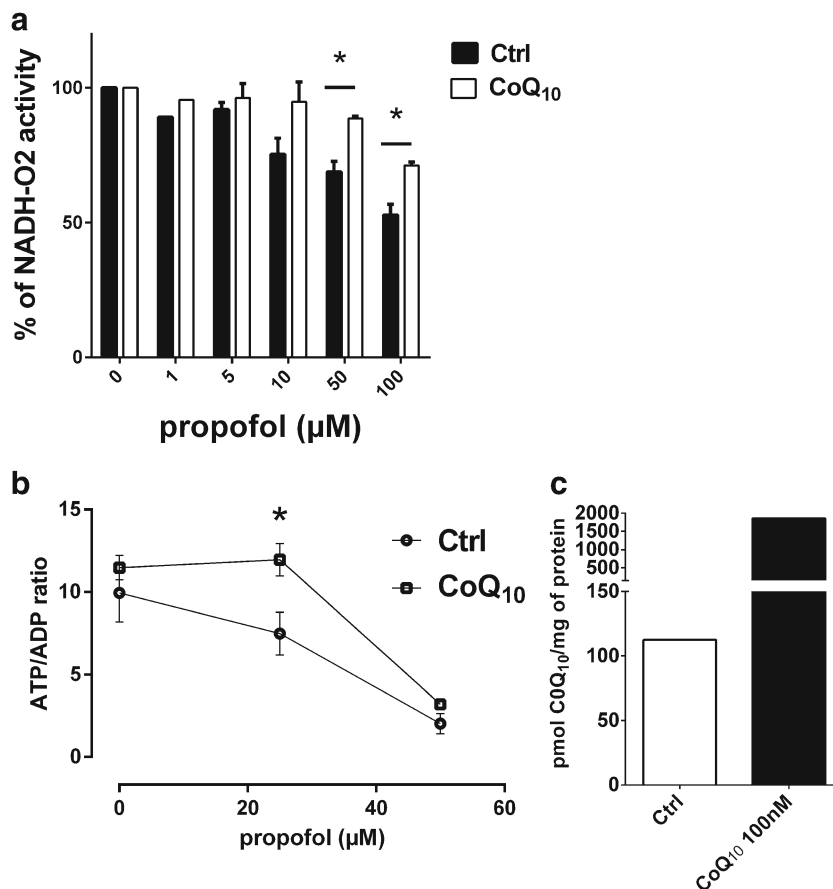
Cell viability was assessed by MTT assay. Data are expressed as percentage of viable cells \pm SE from at least three independent experiments. Significance was determined by t-test analysis between CoQ₁₀-treated and vehicle treated cells (CTRL) * $P \leq 0.05$

Oxygen consumption rate and ATP/ADP rescue

To assess whether the recovery in cell viability could be attributable to the mitochondrial protection due to CoQ₁₀ treatment, we titrated the effect of propofol on oxygen consumption rate and ATP/ADP ratio in cells cultured for 24 h in the presence of 100 nM CoQ₁₀.

Consistently with the viability data, NADH-O₂ reductase activity measured in HeLa cells homogenate exposed to propofol is improved by CoQ₁₀ pre-treatment (Fig. 6a). In line with the latter data, the ATP/ADP ratio (Fig. 6b) is improved in cells pre-treated with CoQ₁₀. Taken together, we showed that a CoQ₁₀ pre-treatment could partially rescue the toxic effect of propofol on the energy profile.

Fig. 6 a-c Protective effect of Coenzyme Q₁₀ on NADH-O₂ activity and ATP/ADP ratio in HeLa cells treated with propofol. Panel a reports the NADH-O₂ activity in HeLa cell homogenate after 5 min of incubation with propofol ranging from 1 to 100 μM. Cells were preincubated for 24 h with 100 nM of terclatrated Coenzyme Q or vehicle (CTRL). Panel b reports the effect of 24 h of propofol treatment on ATP/ADP ratio in HeLa cells preincubated for 24 h with 100 nM of terclatrated Coenzyme Q or vehicle (CTRL). The total amount of cellular coenzyme Q₁₀ after terclatrated Coenzyme Q treatment was detected by HPLC (panel c)



Discussion

A common feature of the propofol effect on cell functions is associated with reduced oxygen consumption that can be correlated to mitochondrial impairment. Considering the crucial role of proper mitochondrial functioning for the neuronal development, it could be argued that these organelles are prominent targets for the toxicity of propofol. Furthermore, the toxic effect of propofol on mitochondrial oxygen consumption is higher in the presence of NADH-dependent substrates, indicating that Complex I is the main target for propofol toxicity (Marian et al. 1997; Schenkman and Yan 2000; Vanlander et al. 2015). The recognition of the mechanism of Complex I inhibition by propofol might be useful to elaborate therapeutic strategies to prevent mitochondrial damage, neurons loss and the long lasting cognitive impairment. Starting from these observations, we analysed the effect of propofol on mitochondrial functionality in two experimental models: cell-free model (BHM) and cultured cells; furthermore we evaluated the protective effect of CoQ₁₀ supplementation in cultured cells. BHM are a suitable model to study the activity of individual respiratory chain enzymes since they can be isolated in large amounts and functionally intact from slaughterhouse material (Pallotti and Lenaz 2007).

We used BHM to identify the main target for propofol toxicity: using specific inhibitors to functionally isolate the different respiratory chain Complexes. We found that propofol affects mainly Complex I. Furthermore, we studied the effect of propofol on the kinetic constants of the enzyme.

Mitochondrial Complex I is one of the most complicated enzyme of the respiratory chain: its structure can be divided into three modules: the dehydrogenase module containing the site for NADH oxidation, the CoQ module responsible for CoQ₁₀ reduction and the proton pumping module completely localized in the membrane arm of the enzyme. The activity of the dehydrogenase module can be distinguished from the activity of CoQ module using as electron acceptor hydrophilic compounds such as [Fe(CN)₆]³⁻ and DCIP. CoQ module activity can be studied using two analogues of the physiological CoQ₁₀ (CoQ₁ and DB). The observed lack of inhibition using ferricyanide and DCIP as electron acceptor allowed to exclude any interaction of propofol with the NADH oxidation site. Moreover the dose dependent effect observed when CoQ₁ and DB were used as electron acceptors indicated that propofol interacts with the CoQ reduction site (Q module) (Brandt 2006).

Moreover, we found that propofol induced a decrease in the catalytic efficiency of Complex I (k_{cat}/K_m) due to a reduction in the maximal velocity (V_{max}) and an increase in the Michaelis-Menten constant (K_m) for quinones. Our results are consistent with a non-competitive inhibition mechanism characterized by the formation of both binary EI and ternary

ESI complexes. The α -parameter for propofol inhibition of the NADH-DB reductase activity is 1 indicating that it has a higher affinity for the free form of the enzyme (E) with respect of the quinone bound form (ES complex).

Although the inhibition mechanism seems to be non-competitive, the increase in the K_m value of Complex I for the quinones, together with the value of the α -parameter, indicate a reduced affinity of the enzyme for the substrate (CoQ). Moreover, the anaesthetic seems to have higher affinity to the free form of the enzyme rather than for the quinone bound form. This last observation offers a starting point to develop a protective strategy based on CoQ₁₀ supplementation. In our previous work we showed that the K_m value for CoQ₁₀ in NADH-Cyt c reductase activity approaches the natural CoQ content of BHM, meaning that Complex I works in non-saturating conditions (Estornell et al. 1992). Thus, in normal conditions, the increase of the mitochondrial ubiquinone content could result in higher oxygen consumption capacity and energy production. While, in conditions in which the enzymes involved in the oxidoreduction of the CoQ pool are damaged (e.g., in the presence of inhibitors) the increase of the mitochondrial ubiquinone content could restore, or at least recover, the normal respiratory capacity and energy production.

In this work, we showed that cultured cells, pretreated with a water-soluble CoQ₁₀ formulation (Q_{Ter}[®]) were more resistant to propofol toxicity, confirming the protective effect of CoQ₁₀.

The rescue of cellular viability is evident at propofol concentrations up to 100 μ M and it is statistically significant at 10 μ M of propofol for T67 cells and 25 μ M for HeLa cells. CoQ₁₀ supplemented cells exposed to propofol showed higher oxygen consumption rate in comparison to controls and the ATP/ADP ratio was maintained for propofol concentrations up to 25 μ M.

Taken together, the results described in this paper show that propofol exposure induces a decrease in the catalytic efficiency of mitochondrial Complex I with a K_i in the micromolar range. Moreover, propofol exposure decreases the cellular energetic charge. The reduced respiratory capacity associated to decreased ATP/ADP ratio could be one of the key mechanisms leading to neuronal damage induced by anaesthesia during early stages of brain development.

The mitochondrial impairment and the effects on the bioenergetics status of cultured cells described in this work were achieved using propofol concentrations ranging between 1 to 100 μ M; in particular, our in vitro study shows that propofol has a significant toxic effect at concentrations of 10–20 μ M.

The relationship between the propofol concentration used in the in vitro study and the concentration used in the clinical practice is an open question. Although it is not easy to verify the intracellular concentration of propofol during anaesthesia, the steady-state blood concentration

during surgical anaesthesia is approximately 4 µg/ml (~22.5 µM) (Kahraman et al. 2008). To the best of our knowledge, this is the first work showing that propofol inhibits one enzyme of the respiratory chain at concentrations comparable with those used in clinical practice.

This study shed light on the molecular process of propofol-induced toxicity and suggest a novel therapeutic strategies that can provide neuroprotection in particular addressed to newborns or infants that have to undergo general anaesthesia.

Acknowledgments The authors thank Professor Giorgio Lenaz M.D., Department of Biomedical and Neuromotor Sciences (DIBINEM), University of Bologna, Italy, for the stimulating discussions and for the critical reading of the paper.

Compliance with ethical standards

Conflict of interest The authors declare that they have no conflict of interest.

Author contributions C.B., N.M., F.V., and L.F. performed experiments, C.B., M.C.M. and R.F. conceived ideas, designed experiments, analysed results. C.B., N.M., J.G. and R.F. wrote the manuscript. All authors edited and reviewed the final manuscript.

References

- Apfelbaum JL, Grasela TH, Hug CC Jr, et al. (1993) The initial clinical experience of 1819 physicians in maintaining anesthesia with propofol: characteristics associated with prolonged time to awakening. *Anesth Analg* 77:S10–S14
- Bercker S, Bert B, Bittigau P, et al. (2009) Neurodegeneration in newborn rats following propofol and Sevoflurane anesthesia. *Neurotox Res* 16:140–147. doi:10.1007/s12640-009-9063-8
- Bergamini C, Moruzzi N, Sblendido A, et al. (2012) A water soluble CoQ10 formulation improves intracellular distribution and promotes mitochondrial respiration in cultured cells. *PLoS One* 7:1–11. doi:10.1371/journal.pone.0033712
- Block RI, Thomas JJ, Bayman EO, et al. (2012) Are anesthesia and surgery during infancy associated with altered academic performance during childhood? *Anesthesiology* 117:494–503. doi:10.1097/ALN.0b013e3182644684
- Boscolo A, Starr JA, Sanchez V, et al. (2012) The abolishment of anesthesia-induced cognitive impairment by timely protection of mitochondria in the developing rat brain: the importance of free oxygen radicals and mitochondrial integrity. *Neurobiol Dis* 45:1031–1041. doi:10.1016/j.nbd.2011.12.022
- Branca D, Vincenti E, Scutari G (1995) Influence of the anesthetic 2, 6-diisopropylphenol (propofol) on isolated rat heart mitochondria. *Comp Biochem Physiol Part C Comp* 110:41–45. doi:10.1016/0742-8413(94)00078-0
- Brandt U (2006) Energy converting NADH:quinone oxidoreductase (complex I). *Annu Rev Biochem* 75:69–92. doi:10.1146/annurev.biochem.75.103004.142539
- Cattano D, Young C, Straiko MMW, Olney JW (2008) Subanesthetic doses of propofol induce neuroapoptosis in the infant mouse brain. *Anesth Analg* 106:1712–1714. doi:10.1213/ane.0b013e318172ba0a
- Cremona T, Kearney EB (1964) Studies on the respiratory chain-linked reduced Nicotinamide adenine dinucleotide dehydrogenase: VI. Further purification and properties of the enzyme from beef heart. *J Biol Chem* 239:2328–2334
- Degli Esposti M, Ghelli A, Ratta M, et al. (1994) Natural substances (acetogenins) from the family Annonaceae are powerful inhibitors of mitochondrial NADH dehydrogenase (Complex I). *Biochem J* 301(Pt 1):161–167. doi:10.1016/j.bmcl.2003.11.021
- Dobbing J, Sands J (1979) Comparative aspects of the brain growth spurt. *Early Hum Dev* 3:79–83. doi:10.1016/0378-3782(79)90022-7
- Driessen J, Willems S, Dercksen S, et al. (2007) Anesthesia-related morbidity and mortality after surgery for muscle biopsy in children with mitochondrial defects. *Paediatr Anaesth* 17:16–21. doi:10.1111/j.1460-9592.2006.02043.x
- Estabrook RW (1967) Mitochondrial respiratory control and the polarographic measurement of ADP:O ratios. *Methods Enzymol* 10:41–47. doi:10.1016/0076-6879(67)10010-4
- Estornell E, Fato R, Castelluccio C, et al. (1992) Saturation kinetics of coenzyme Q in NADH and succinate oxidation in beef heart mitochondria. *FEBS Lett* 311:107–109. doi:10.1016/0014-5793(92)81378-Y
- Estornell E, Fato R, Pallotti F, Lenaz G (1993) Assay conditions for the mitochondrial NADH:coenzyme Q oxidoreductase. *FEBS Lett* 332:127–131. doi:10.1016/0014-5793(93)80498-J
- Fato R, Estornell E, Di Bernardo S, et al. (1996) Steady-state kinetics of the reduction of coenzyme Q analogs by complex I (NADH:ubiquinone oxidoreductase) in bovine heart mitochondria and submitochondrial particles. *Biochemistry* 35:2705–2716. doi:10.1021/bi9516034
- Fato R, Bergamini C, Bortolus M, et al. (2009) Differential effects of mitochondrial complex I inhibitors on production of reactive oxygen species. *Biochim Biophys Acta* 1787:384–392. doi:10.1016/j.bbabi.2008.11.003
- Fetoni AR, De Bartolo P, Eramo SLM, et al. (2013) Noise-induced hearing loss (NIHL) as a target of oxidative stress-mediated damage: cochlear and cortical responses after an increase in antioxidant defense. *J Neurosci* 33:4011–4023. doi:10.1523/JNEUROSCI.2282-12.2013
- Fodale V, La Monaca E (2008) Propofol infusion syndrome: an overview of a perplexing disease. *Drug Saf* 31:293–303
- Fredriksson A, Archer T, Alm H, et al. (2004) Neurofunctional deficits and potentiated apoptosis by neonatal NMDA antagonist administration. *Behav Brain Res* 153:367–376. doi:10.1016/j.bbr.2003.12.026
- Fredriksson A, Pontén E, Gordh T, Eriksson P (2007) Neonatal exposure to a combination of N-methyl-D-aspartate and gamma-aminobutyric acid type A receptor anesthetic agents potentiates apoptotic neurodegeneration and persistent behavioral deficits. *Anesthesiology* 107:427–436. doi:10.1097/01.aoa.0000308309.23565.70
- Gornall AG, Bardawill CJ, David MM (1949) Determination of serum proteins by means of the biuret reaction. *J Biol Chem* 177:751–766
- Haase R, Sauer H, Eichler G (2005) Lactic acidosis following short-term propofol infusion may be an early warning of propofol infusion syndrome. *J Neurosurg Anesthesiol* 17:122–123
- Istaphanous GK, Loepke AW (2009) General anesthetics and the developing brain. *Curr Opin Anaesthesiol* 22:368–373. doi:10.1097/ACO.0b013e3283294c9e
- Javadov SA, Lim KH, Kerr PM, et al. (2000) Protection of hearts from reperfusion injury by propofol is associated with inhibition of the mitochondrial permeability transition. *Cardiovasc Res* 45:360–369
- Jevtovic-Todorovic V, Hartman RE, Izumi Y, et al. (2003) Early exposure to common anesthetic agents causes widespread neurodegeneration in the developing rat brain and persistent learning deficits. *J Neurosci* 23:876–882. doi:10.1097/00008506-200307000-00029

- Jones D (1981) Determination of pyridine dinucleotides in cell extracts by high-performance liquid chromatography. *J Chromatogr* 225:446–449
- Kahraman S, Zup SL, McCarthy MM, Fiskum G (2008) GABAergic mechanism of propofol toxicity in immature neurons. *J Neurosurg Anesthesiol* 20:233–240. doi:10.1097/ANA.0b013e31817ec34d
- Koch M, De Backer D, Vincent J (2004) Lactic acidosis: an early marker of propofol infusion syndrome? *Intensive Care Med* 30:522
- Lauro GM, Di Lorenzo N, Grossi M, et al. (1986) Prostaglandin E2 as an immunomodulating factor released in vitro by human glioma cells. *Acta Neuropathol* 69:278–282. doi:10.1007/BF00688305
- Leskovic V (2003) Comprehensive enzyme kinetics. Publisher Springer US, Copyright Springer Science+Business Media, New York
- Marian M, Parrino C, Leo AM, et al. (1997) Effect of the intravenous anesthetic 2,6-diisopropylphenol on respiration and energy production by rat brain synaptosomes. *Neurochem Res* 22:287–292. doi:10.1023/A:1022438805337
- Pallotti F, Lenaz G (2007) Isolation and Subfractionation of mitochondria from animal cells and tissue culture lines. *Methods Cell Biol* 80:3–44
- Parke TJ, Stevens JE, Rice AS, et al. (1992) Metabolic acidosis and fatal myocardial failure after propofol infusion in children: five case reports. *BMJ* 305:613–616. doi:10.1136/bmj.305.6854.613
- Paule MG, Li M, Allen RR, et al. (2011) Ketamine anesthesia during the first week of life can cause long-lasting cognitive deficits in rhesus monkeys. *Neurotoxicol Teratol* 33:220–230. doi:10.1016/j.ntt.2011.01.001
- Pearm ML, Fellow Postdoctoral, Hu Y, et al. (2012) Propofol neurotoxicity is mediated by p75 neurotrophin receptor activation. *Anesthesiology* 116:352–361. doi:10.1097/ALN.0b013e318242a48c
- Schenkman KA, Yan SL (2000) Propofol impairment of mitochondrial respiration in isolated perfused Guinea pig hearts determined by reflectance spectroscopy. *Crit Care Med* 28:172–177. doi:10.1097/00003246-200001000-00028
- Schwartz D, Raghunathan K (2009) Anesthesia and mitochondrial disorders. *Paediatr Anaesth* 19:60–61
- Sebel P, Lowdon J (1989) Propofol: a new intravenous anesthetic. *Anesthesiology* 71:260–277
- Smith AL (1967) 13] preparation, properties, and conditions for assay of mitochondria: slaughterhouse material, small-scale. *Methods Enzymol* 10:81–86. doi:10.1016/0076-6879(67)10016-5
- Smith S, Cottingham I, Ragan C (1980) Immunological assays of the NADH dehydrogenase content of bovine heart mitochondria and submitochondrial particles. *FEBS Lett* 110:279–282
- Stratmann G (2011) Neurotoxicity of anesthetic drugs in the developing brain. *Anesth Analg* 113:1170–1179
- Sztark F, Ichas F, Ouhabi R, et al. (1995) Effects of the anaesthetic propofol on the calcium-induced permeability transition of rat heart mitochondria: direct pore inhibition and shift of the gating potential. *FEBS Lett* 368:101–104. doi:10.1016/0014-5793(95)00610-L
- Takada M, Ikenoya S, Yuzuriha T, Katayama K (1984) Simultaneous determination of reduced and oxidized ubiquinones. *Methods Enzymol* 105:147–155
- Twaroski DM, Yan Y, Zaja I, et al. (2015) Altered mitochondrial dynamics contributes to propofol-induced cell death in human stem cell-derived neurons. *Anesthesiology* 123:1067–1083. doi:10.1097/ALN.0000000000000857
- Vanlander AV, Okun JG, de Jaeger A, Smet J, De Lattre E, et al. (2015) Possible pathogenic mechanism of propofol infusion syndrome involves coenzyme q. *Anesthesiology* 122:343–352
- Wilder RT, Flick RP, Sprung J, et al. (2009) Early exposure to anesthesia and learning disabilities in a population-based birth cohort. *Anesthesiology* 110:796–804. doi:10.1097/01.anes.0000344728.34332.5d
- Wolf A, Weir P, Segar P, et al. (2001) Impaired fatty acid oxidation in propofol infusion syndrome. *Lancet* 357:606–607. doi:10.1016/S0140-6736(00)04064-2
- Wu, GJ, Tai YT, Chen TL, et al (2005) Propofol specifically inhibits mitochondrial membrane potential but not complex I NADH dehydrogenase activity, thus reducing cellular ATP biosynthesis and migration of macrophages. *Ann N Y Acad Sci* 168–176
- Zou W-W, Xiao H-P, M-N G, et al. (2013) Propofol induces rat embryonic neural stem cell apoptosis by activating both extrinsic and intrinsic pathways. *Mol Med Rep* 7:1123–1128. doi:10.3892/mmr.2013.1298